Investigation of Rotor Performance and Loads of a UH-60A Individual Blade Control System

Hyeonsoo Yeo
Aeroflightdynamics Directorate (AMRDEC)
U.S. Army Research, Development, and Engineering Command
Ames Research Center, Moffett Field, California

Ethan A. Romander
Thomas R. Norman
Flight Vehicle Research and Technology Division
NASA Ames Research Center
Moffett Field, California

Abstract for the American Helicopter Society 66th Annual Forum
May 11-13, 2010
Phoenix, AZ

A full-scale wind tunnel test was recently conducted (March 2009) in the National Full-Scale Aerodynamics Complex (NFAC) 40- by 80-Foot Wind Tunnel to evaluate the potential of an individual blade control (IBC) system to improve rotor performance and reduce vibrations, loads, and noise for a UH-60A rotor system [1]. This test was the culmination of a long-term collaborative effort between NASA, U.S. Army, Sikorsky Aircraft Corporation, and ZF Luftfahrttechnik GmbH (ZFL) to demonstrate the benefits of IBC for a UH-60A rotor. Figure 1 shows the UH-60A rotor and IBC system mounted on the NFAC Large Rotor Test Apparatus (LRTA).

The IBC concept used in the current study utilizes actuators placed in the rotating frame, one per blade. In particular, the pitch link of the rotor blade was replaced with an actuator, so that the blade root pitch can be changed independently. This concept, designed for a full-scale UH-60A rotor, was previously tested in the NFAC 80- by 120-Foot Wind Tunnel in September 2001 at speeds up to 85 knots [2]. For the current test, the same UH-60A rotor and IBC system were tested in the 40- by 80-Foot Wind Tunnel at speeds up to 170 knots. Figure 2 shows the servo-hydraulic IBC actuator installed between the swashplate and the blade pitch horn.

Although previous wind tunnel experiments [3, 4] and analytical studies on IBC [5, 6] have shown the promise to improve the rotor's performance, in-depth correlation studies have not been performed. Thus, the current test provides a unique resource that can be used to assess the accuracy and reliability of prediction methods and refine theoretical models, with the ultimate goal of providing the technology for timely and cost-effective design and development of new rotors.

In this paper, rotor performance and loads calculations are carried out using the analyses CAMRAD II and coupled OVERFLOW-2/CAMRAD II and the results are compared with these UH-60A/IBC wind tunnel test data.

First, the analytical results were obtained using the comprehensive analysis CAMRAD II [7], which has been used extensively for correlation of performance and loads measurements of UH-60A in various flight conditions [8–11]. The trim method performed in the test (and current analysis) specified the rotor lift, propulsive force and hub rolling moment with the rotor shaft angle of attack fixed. The hub pitching moment was not controlled or used for feedback. This trim control method is very efficient as the rotor propulsive force was not controlled through the change to the model shaft angle of attack. The rotor was re-trimmed with each IBC input in order to make sure that the rotor was

operating at the same conditions with and without IBC excitation.

Figures 3 and 4 show the effects of 2/rev IBC on the main rotor power at the advance ratio of 0.35 and 0.40, respectively. Calculated main rotor power and delta main rotor power are compared with the measured values at various IBC phase angles. The test conditions are $C_L/\sigma = 0.0766, C_X/\sigma = 0.0092, C_{mx}/\sigma = 0.0092, \mu = 0.35, \alpha_s = -6.94^\circ$ and $C_L/\sigma = 0.0766, C_X/\sigma = 0.0085, \mu = 0.40, \alpha_s = -8.25^\circ$, respectively. The wind tunnel wall correction, in the form of the induced angle correction, is used to correct the 40 x 80 rotor lift and rotor propulsive force at the various physical rotor shaft angles, thrust, and advance ratios. The test conditions shown above are corrected values. It should be noted that the propulsive force at μ = 0.4 is smaller than that at μ = 0.35 because of control limitations. The measured data show that the 1.5 deg IBC actuation reduced main rotor power by 3.4% and 5.1% at μ = 0.35 and 0.40, respectively. The optimum phase angle is 225 deg for both cases. The calculated main rotor power shows very good correlation with the measured values at μ = 0.35. However, an underprediction of power is observed at μ = 0.40. The analysis underpredicts the effect of IBC on power reduction. The calculated power reductions are 2.0% and 1.9% at μ = 0.35 and 0.40, respectively, and the optimum phase is 210 deg for both cases.

Figure 5 compares the calculated flap and chord bending moments and IBC actuator force (pitch link force) with the measured values. Steady values are removed from both test data and analysis, so that only oscillatory components are compared. The test condition is $C_L/\sigma = 0.0766, C_X/\sigma = 0.0092, C_{mx}/\sigma = 0.0092, \mu = 0.35, \alpha_s = -6.94^\circ$ and no IBC actuation was applied. Figure 5(a) shows the oscillatory flap bending moment at 40% radial station. The analysis shows reasonably good correlation on magnitude, but the phase differs. This phase difference was also observed in the comparison with flight test data [11]. Figure 5(b) shows the oscillatory chord bending moment at 40% radial station. A linear lag damper model was used in the current calculation. However, a nonlinear model will be incorporated to improve the correlation. The chord bending moment is expected to be influenced by the lag damper force at this location. Figure 5(c) shows the oscillatory IBC actuator force. The analysis underpredicts the amplitude and was not able to capture the waveform on the retreating side.

CAMRAD II uses a lower-fidelity aerodynamics model than that available in modern Computational Fluid Dynamics (CFD) codes, and most CFD codes lack the sophisticated Computational Structural Dynamics (CSD) and trim capabilities of comprehensive codes like CAMRAD II. Coupling a CFD code (e.g. OVERFLOW-2) to a comprehensive code (e.g. CAMRAD II) marries the strengths of the two approaches and produces the highest-fidelity solution currently possible. Coupling is achieved by alternate execution of OVERFLOW and CAMRAD II. At the end of each code's "turn" to execute, it passes data to the next code. The data passed from OVERFLOW to CAMRAD II is airload data integrated from its Navier-Stokes model of the UH-60 rotor. This airload data is used to correct CAMRAD II's internal aerodynamics model (which consists of airfoil tables and a lower-order wake model) (Fig. 6). At the end of its execution, CAMRAD II generates updated control positions and a description of how the blade deforms as it revolves around the shaft. These quantities are used to give OVERFLOW's grids a realistic motion in response to the aerodynamic environment (Fig. 7). Potsdam et al. [12] demonstrated improved airloads prediction capability for the UH-60A rotor using a loosely coupled CFD/CSD method in steady level flight conditions.

It is expected that the coupled simulation will provide increased accuracy in predicting the IBC power increment by increasing the fidelity of the rotor's aerodynamic environment. This is especially important in flow regimes where CAMRAD II has difficulty accurately modeling blade aerodynamics (e.g. dynamic stall) or wake geometry (e.g. low advance ratio). Prior calculations have identified differences between coupled calculations and those using CAMRAD II alone as shown in Fig. 8. It should be noted that these calculations were performed prior to the test using different operating conditions and trim strategies and thus offer little evidence to suggest which simulation is more accurate.

In the final paper, rotor performance and loads will be calculated using the comprehensive analysis CAMRAD II and coupled OVERFLOW-2/CAMRAD II and the results will be compared with the wind tunnel measurements at various speeds and thrusts, with different IBC actuation magnitudes and phases. Also investigated will be the influence of OVERFLOW-2's grid density, numerical scheme, and turbulence model on the accuracy of the coupled calculation.

References

[1] Norman, T. R., Theodore, C., Shinoda, P. M., Fuerst, D., Arnold, U. T. P., Makinen, S., Lorber, P., and O'Neill, J., "Full-scale Wind Tunnel Test of a UH-60 Individual Blade Control System for Performance Improvement and Vibration, Loads, and Noise Control," American Helicopter Society 65th Annual Forum Proceedings, Grapevine, TX, May 27-29, 2009.

[2] Norman, T. R., Shinoda, P. M., Kitaplioglu, C., Jacklin, S. A., and Sheikman, A., "Low-Speed Wind Tunnel Investigation of a Full-Scale UH-60 Rotor System," American Helicopter Society 58th Annual Forum Proceedings, Montreal, Canada, June 2002.

[3] Jacklin, S. A., Blaas, A., Teves, D., and Kube, R., "Reduction of Helicopter BVI Noise, Vibration, and Power Consumption through Individual Blade Control," American Helicopter Society 51st Annual Forum Proceedings, Fort Worth, TX, May 1995.

[4] Lorber, P. F., Park, C., Polak, D., O'Neill, J., and, Welsh, W., "Active Rotor Experiments at Mach Scale Using Root Pitch IBC," American Helicopter Society 57th Annual Forum Proceedings, Washington D.C., May 2001.

[5] Cheng, R. P., and Celi, R., "Optimum Two-Per-Revolution Inputs for Improved Rotor Performance," *Journal of Aircraft*, Vol. 42, No. 6, November-December 2005, pp. 1409-1417.

[6] Yeo, H., "Assessment of Active Controls for Rotor Performance Enhancement," *Journal of the American Helicopter Society*, Vol. 53, (2), April 2008, pp. 152- 163.

[7] Johnson, W., "Technology Drivers in the Development of CAMRAD II," American Helicopter Society Aeromechanics Specialist Meeting, San Francisco, CA, January 1994.

[8] Yeo, H., Bousman, W. G., and Johnson, W., "Performance Analysis of a Utility Helicopter with Standard and Advanced Rotor," *Journal of the American Helicopter Society*, Vol. 49, No. 3, July 2004, pp. 250-270.

[9] Shinoda, P. M., Yeo. H., and Norman, T. R., "Rotor Performance of a UH-60 Rotor System in the NASA Ames 80- by 120-Foot Wind Tunnel," *Journal of the American Helicopter Society*, Vol. 49, No. 4, October 2004.

[10] Yeo, H., and Johnson, W., "Assessment of Comprehensive Analysis Calculation of Airloads on Helicopter Rotors," *Journal of Aircraft*, Vol. 42, No. 5, September-October 2005.

[11] Yeo, H., and Johnson, W., "Prediction of Rotor Structural Loads with Comprehensive Analysis," *Journal of the American Helicopter Society*, Vol. 53, No. 2, April 2008.

[12] Potsdam, M., Yeo, H., and Johnson, W., "Rotor Airloads Prediction Using Loose Aerodynamic/Structural Coupling," *Journal of Aircraft*, Vol. 43, No. 3, May-June 2006.

Figure 1: UH-60A rotor system installed on the Large Rotor Test Apparatus in the NFAC 40-by 80-Foot Wind Tunnel.

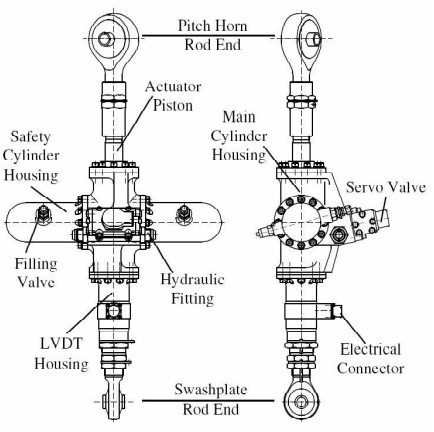

(a) IBC actuator schematic.

(b) IBC actuator installed on UH-60A rotor.

Figure 2: IBC actuator.

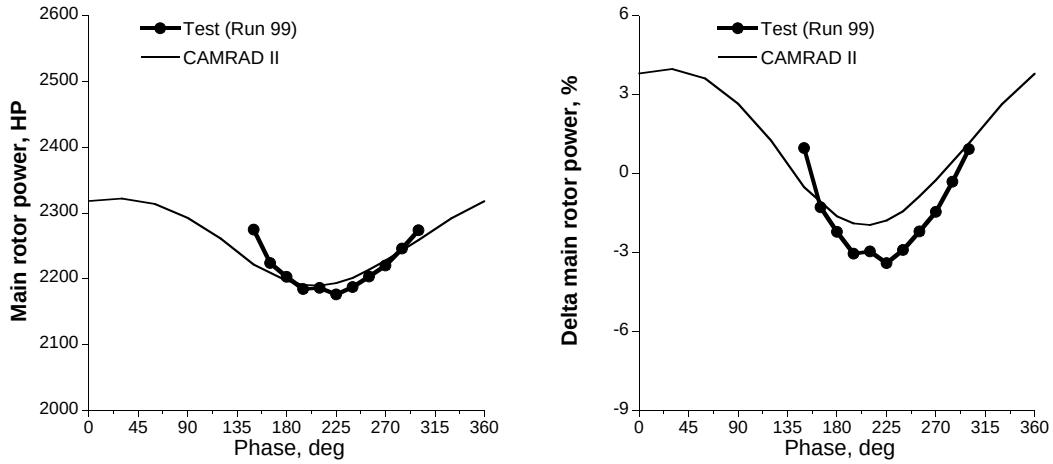

Figure 3: Main rotor power from 2/rev IBC phase sweep (1.5° amplitude), $C_L/\sigma = 0.0766, C_X/\sigma = 0.0092, \mu = 0.35, \alpha_s = -6.94°$

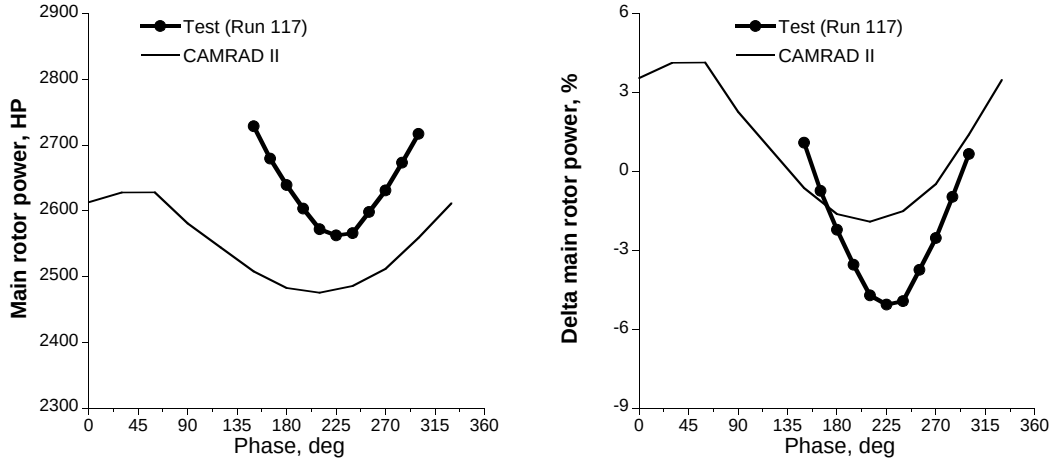

Figure 4: Main rotor power from 2/rev IBC phase sweep (1.5° amplitude), $C_L/\sigma = 0.0766, C_X/\sigma = 0.0085, \mu = 0.40, \alpha_s = -8.25°$

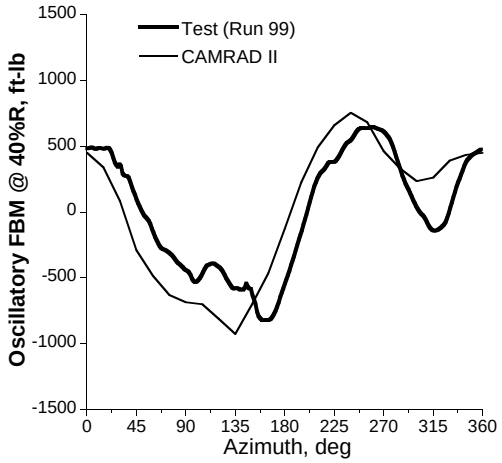

(a) Flap bending moment at 40%R

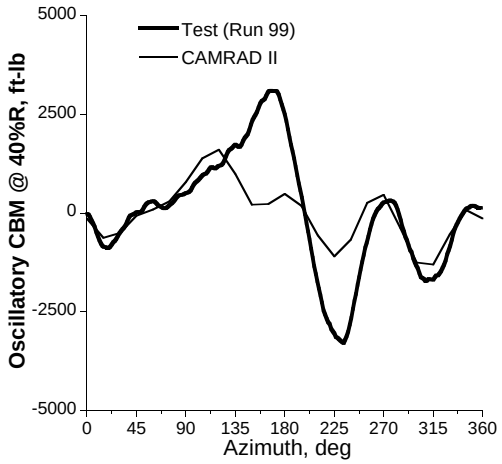

(b) Chord bending moment at 40%R

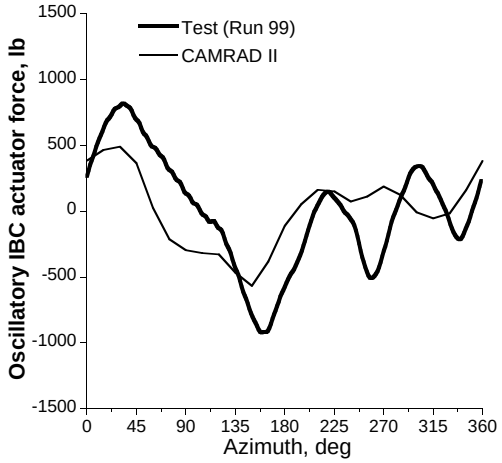

(c) IBC actuator force

Figure 5: Oscillatory rotor loads without IBC (baseline), $C_L/\sigma = 0.0766, C_X/\sigma = 0.0092, \mu = 0.35, \alpha_s = -6.94^\circ$

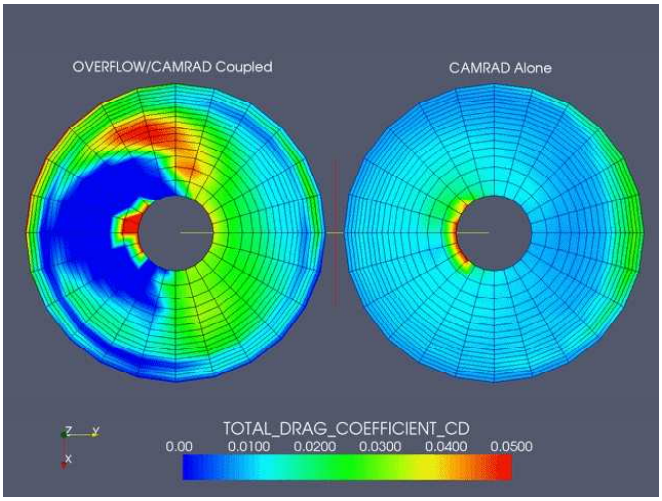

Figure 6: Comparison of aerodynamic models: CAMRAD II corrected with airloads from OVERFLOW-2 (left), uncorrected CAMRAD II (right).

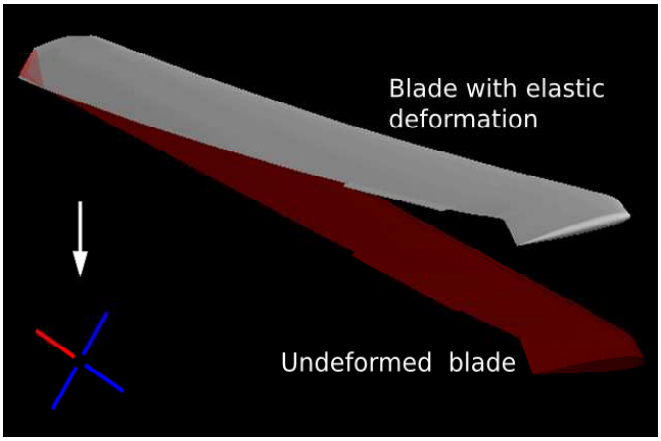

Figure 7: Deformed CFD grid compared to rigid model. μ=0.325; T=18k lb.

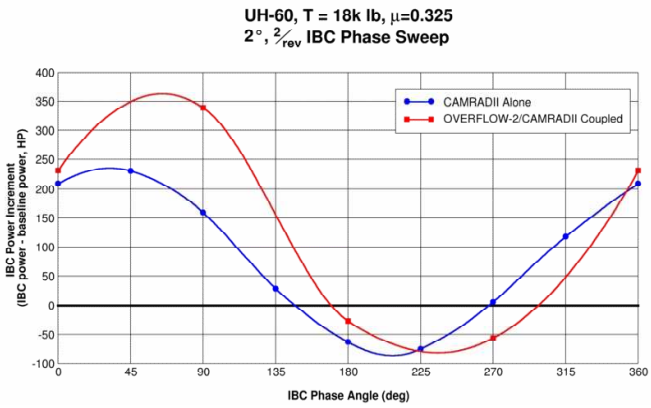

Figure 8: The effect of IBC input on required power as computed by CAMRAD II alone (blue) and CAMRAD II coupled to OVERFLOW-2 (red).